Molecular and Cellular Reports A Pharmacological Study of the Action of Esculetin on Human Prostate Cancer Cells

Chung-Ren Jan (crjan@isca.vghks.gov.tw)
Kaohsiung Veterans General Hospital https://orcid.org/0000-0003-2805-8418
Jue-Long Wang
Kaohsiung Veterans General Hospital
Wei-Chuan Liao
Kaohsiung Veterans General Hospital
Rong-An Lin
Kaohsiung Veterans General Hospital Tainan Branch
Shu-Han Chang
Kaohsiung Medical University
Chun-Chi Kuo
Tzu Hui Institute of Technology
Lyh-Jyh Hao
Kaohsiung Veterans General Hospital Tainan Branch
Chiang-Ting Chou
Chang Gung University of Science and Technology College of Nursing

Research Article

Keywords: Ca2+, Fura-2, Prostate Cells, Esculetin

Posted Date: September 22nd, 2021

DOI: https://doi.org/10.21203/rs.3.rs-893922/v1

Abstract

Esculetin is a derivative of coumarin, and is the dominant, vigorous component of the conventional Chinese medicine *Cortex Fraxini*. Recently, the molecular pathway study and clinical use of *Cortex Fraxini* and esculetin are becoming intensive. In vitro, esculetin has been shown to provoke apoptotic responses via mitochondrial routes and other cellular responses in diverse cell types. The action of esculetin on cytosolic Ca^{2+} concentration ($[Ca^{2+}]_i$) in prostate cells is unknown. $[Ca^{2+}]_i$ were assayed by applying fura-2, a fluorescent Ca^{2+}-sensitive probe. WST-1 was used to measure cell death. Esculetin at doses of 25–100 μM provoked $[Ca^{2+}]_i$ raises. Removing external Ca^{2+} decreased the response by 15%. Esculetin (100 μM) provoked Mn^{2+} entry implying Ca^{2+} influx. Esculetin-provoked Ca^{2+} influx was suppressed by half by protein kinase C (PKC) activator (phorbol 12-myristate 13 acetate, PMA) and inhibitor (GF109203X); and by three inhibitors of store-operated Ca^{2+} channels: nifedipine, econazole and SKF96365. In the absence of Ca^{2+}, pretreatment with the endoplasmic reticulum (ER) Ca^{2+} pump suppressor thapsigargin completely suppressed esculetin-provoked $[Ca^{2+}]_i$ raises. Suppression of phospholipase C (PLC) with U73122 eliminated esculetin-provoked $[Ca^{2+}]_i$ raises. Esculetin at 20–70 μM caused death of cells, which was not prevented by incubation with the Ca^{2+} binder 1,2-bis(2-aminophenoxy)ethane-N,N,N',N'-tetraacetic acid-acetoxymethyl ester (BAPTA/AM). In sum, in PC3 prostate cells, esculetin provoked $[Ca^{2+}]_i$ raises by provoking PLC-associated Ca^{2+} discharge from ER and Ca^{2+} influx via PKC-sensitive store-operated Ca^{2+} influx. Additionally, esculetin provoked Ca^{2+}-dissociated cell death.

Introduction

Esculetin is a derivative of coumarin, and is the major vigorous component of the conventional Chinese medicine *Cortex Fraxini*. Recently, the in vitro pathways study and clinical use of *Cortex Fraxini* and esculetin become intense [1]. In vitro, apoptosis and other cellular responses in diverse cell types have been shown to be induced by esculetin [2]. Esculetin was shown to evoke apoptotic pathways of SMMC-7721 cells [3], suppress lung cancer by inhibiting protein expression [4], and regulate cell viability provoked by oxidants in leukemia cells [5].

Furthermore, data show that esculetin exhibits inhibitory action on human gastric cancer involving IGF-1 related signaling routes [6], suppresses prostate cancer cells by provoking apoptosis [7], induces apoptotic processes in pancreatic cancer cells by chelating KEAP1 [8], and evokes human colon cancer cell death via mitochondrial apoptotic pathways [9].

There was only one paper described the effect of esculetin on $[Ca^{2+}]_i$ and viability in breast cancer cells [10]. Thus it appears necessary to study the action of esculetin on signal transduction and its pertinent physiology in all cell types.

Ca^{2+} is a special cation in physiology. It is a crucial second messenger responsible for modulating many cellular responses including fertilization, apoptosis, energy transduction, protein activation, fluid

secretion, muscle contraction and enzyme activation [11]. In unstimulated cells, the cytosolic free level of Ca^{2+} ($[Ca^{2+}]_i$) is controlled at 50–100 nM while the external Ca^{2+} concentration was 2 mM [12]. A Ca^{2+} response is provoked by Ca^{2+} entry from external medium or Ca^{2+} discharge through internal depots [13]. In many cells, the store-operated Ca^{2+} entry plays a dominant part in Ca^{2+} entry [14]. ER can release stored Ca^{2+} through phosphiolipase C-mediated processes or suppression of ER Ca^{2+} ATP pumps [15]. Ca^{2+} signal interacts with many other cytosolic messengers such as cGMP, cAMP, and protein kinases [16]. The influence of esculetin on $[Ca^{2+}]_i$ is unclear in prostate cells. Because a Ca^{2+} signal can trigger numerous cellular responses, it is crucial to unveil the mechanisms of esculetin-caused $[Ca^{2+}]_i$ raises to know the pharmacology of esculetin in prostate cells.

Materials And Methods

Chemicals

The chemicals used for cell culture were from Gibco® (Gaithersburg, MD, USA). Aminopolycarboxylic acid/acetoxy methyl (fura-2/AM) and 1,2-bis(2-aminophenoxy)ethane-N,N,N',N'-tetraacetic acid/acetoxy methyl (BAPTA/AM) were from Molecular Probes® (Eugene, OR, USA). All other chemicals were from Sigma-Aldrich® (St. Louis, MO, USA).

Cell culture

PC3 human prostate cancer cells are purchased from Bioresource Collection and Research Center (Taiwan). Cells were cultured in RPMI-1640 medium. The medium had penicillin (100 units/mL)-streptomycin (100 μg/mL) and fetal bovine serum (10%) kept at 37°C in a humidified 5% CO_2 atmosphere.

Solutions used in $[Ca^{2+}]_i$ measurements

Ca^{2+}-containing medium (pH 7.4) contained 140 mM NaCl, 5 mM KCl, 1 mM $MgCl_2$, 2 mM $CaCl_2$, 10 mM 4-(2-hydroxyethyl)-1-piperazineethanesulfonic acid (HEPES), and 5 mM glucose. Ca^{2+}-free medium contained similar chemicals as Ca^{2+}-containing medium except that $CaCl_2$ was replaced with 0.3 mM ethylene glycol tetraacetic acid (EGTA) and 2 mM $MgCl_2$. Esculetin was dissolved in ethanol as a 0.1 M stock solution. The other chemicals were dissolved in water, ethanol or dimethyl sulfoxide (DMSO). The concentration of solvents in the experimental solutions did not exceed 0.1%, and did not affect viability or basal $[Ca^{2+}]_i$.

$[Ca^{2+}]_i$ analyses

Cells grew to confluency on 6 cm dishes were trypsinized and made into a suspension in culture medium at a concentration of $10^6 mL^{-1}$. Trypan blue exclusion was used to determine cell viability. After the treatment, the viability was greater than 95%. Then cells were loaded with 2 μM fura-2/AM for 30 min at

25°C in the same medium. Afterwards, cells were washed with Ca^{2+}-containing medium twice and were made into a suspension in Ca^{2+}-containing medium at a concentration of $10^7 mL^{-1}$. Fura-2 fluorescence measurements were performed in a water-jacketed cuvette (25°C) with continuous stirring; the cuvette had 1 mL of medium and 0.5 million cells. Fluorescence was monitored with a Shimadzu RF-5301PC spectrofluorophotometer immediately after 0.1 mL cell suspension was added to 0.9 mL Ca^{2+}-containing or Ca^{2+}-free medium, by recording excitation signals at 340 nm and 380 nm and emission signal at 510 nm at 1-s intervals. During the recording, reagents (PMA (1 nM); GF109203X (2 μM); econazole (0.5 μM), nifedipine (1 μM), SKF96365 (5 μM), thapsigargin (1 μM), U73122 (2 μM), or ATP (4 μM)) were administered to the cuvette by pausing the recording for 3 s to open and close the chamber) were added to the cuvette by pausing the recording for 2 s to open and close the cuvette-containing chamber. After completion of the experiments, the detergent Triton X-100 (0.1%) and $CaCl_2$ (5 mM) were added to the cuvette to obtain the maximal fura-2 fluorescence; then the Ca^{2+} chelator EGTA (10 mM) was added to chelate Ca^{2+} in the cuvette to obtain the minimal fura-2 fluorescence for calibration of $[Ca^{2+}]_i$ after 20 min of fluorescence measurements. Control experiments showed that cells bathed in a cuvette had a viability of 95%. $[Ca^{2+}]_i$ was calculated as described previously [17]. Mn^{2+} smothering of fura-2 fluorescence was performed in Ca^{2+}-containing medium containing 50 μM $MnCl_2$. $MnCl_2$ was added to cell suspension in the cuvette 30 s before the fluorescence recording was started. Data were recorded at excitation signal at 360 nm (Ca^{2+}-insensitive) and emission signal at 510 nm at 1-s intervals as described previously [18].

Cell viability assays

Cell viability measurements were based on the ability of cells to cleave tetrazolium salts by dehydrogenases. Increases in the intensity of color correlated with the number of live cells. Assays were conducted based on manufacturer's instructions (Roche Molecular Biochemical, Indianapolis, IN, USA). Cells were seeded in 96-well plates at a concentration of 10^4 cells/well in culture medium for 24 h in the presence of 0–70 μM esculetin. The cell viability detecting tetrazolium reagent 4-[3-[4-Iodophenyl]-2-4(4-nitrophenyl)-2H-5-tetrazolio-1,3-benzene disulfonate] (WST-1; 10 μL pure solution) was added to samples after esculetin treatment, and cells were incubated for 30 min in a humidified atmosphere. In experiments using BAPTA/AM to chelate cytosolic Ca^{2+}, cells were treated with 5 μM BAPTA/AM for 1 h before esculetin (0–70 μM) incubation. The cells were washed once with Ca^{2+}-containing medium and incubated with or without esculetin for 24 h. The absorbance of samples (A_{450}) was analyzed using an enzyme-linked immunosorbent assay (ELISA) reader. Absolute optical density was normalized to the absorbance of unstimulated cells in each plate and expressed as a percentage of the control value.

Statistics

Data are reported as mean ± SEM (standard error of the mean) of three separate assays and were analyzed by one-way analysis of variances (ANOVA) using the Statistical Analysis System (SAS®, SAS Institute Inc., Cary, NC, USA). Multiple comparisons between group means were performed by *post-hoc*

analysis using the Tukey's HSD (honestly significantly difference) procedure. A *P*-value less than 0.05 were considered significant.

Results

Chemical structure of esculetin

Figure 1 shows the structure of esculetin.

Esculetin-provoked $[Ca^{2+}]_i$ raises

The action of esculetin on resting $[Ca^{2+}]_i$ was investigated. Figure 2(**a**) depicts resting $[Ca^{2+}]_i$ was 50 ± 2 nM. At 25–100 μM, esculetin provoked $[Ca^{2+}]_i$ raises in a dose-associated fashion in Ca^{2+}-containing solution. At 100 μM, esculetin provoked $[Ca^{2+}]_i$ raises that reached 51 ± 2 nM. The Ca^{2+} signal reached saturation at 100 μM esculetin since at 150 μM, esculetin provoked a comparable action as that provoked by 100 μM esculetin (unshown). Figure 2(**b**) illustrates in the absence of Ca^{2+}, 25–100 μM esculetin induced dose-associated raises in $[Ca^{2+}]_i$. Figure 2(**c**) depicts the dose-signal relationships of esculetin-provoked $[Ca^{2+}]_i$ raises. The EC_{50} was 65 ± 1 μM in the presence of Ca^{2+} or 40 ± 2 μM in the absence of Ca^{2+}, correspondingly. These were obtained by fitting to Hill equations. In Ca^{2+}-free solution, esculetin-provoked $[Ca^{2+}]_i$ raises were reduced by approximately 15%.

Esculetin-provoked Mn^{2+} entry

Assays were conducted to verify esculetin-provoked $[Ca^{2+}]_i$ raises included Ca^{2+} entry. Mn^{2+} and Ca^{2+} get into cells through comparable routes but Mn^{2+} smothered fluorescence at all excitation wavelengths [18]. Hence, smothering of fura-2 fluorescence excited at the Ca^{2+}-insensitive excitation wavelength of 360 nm by Mn^{2+} suggests Ca^{2+} entry. Since esculetin-provoked Ca^{2+} signal reached saturation at 100 μM, in the next set of assays the Ca^{2+} signal provoked by 100 μM esculetin was chosen as control. Figure 3 implied that 100 μM esculetin provoked an immediate reduction in the 360 nm excitation recording that attained to a maximum of 120 ± 2 random units at 75 s. The findings implicated that Ca^{2+} entry was involved in esculetin-provoked $[Ca^{2+}]_i$ raises.

The routes of esculetin-provoked Ca^{2+} influx

Assays were performed to dissect the Ca^{2+} influx routes of esculetin-provoked $[Ca^{2+}]_i$ raises. Nifedipine and the store-operated Ca^{2+} entry inhibitors: econazole (0.5 μM) and SKF96365 (5 μM); phorbol 12-myristate 13 acetate (PMA; 1 nM; a protein kinase C [PKC] activator); and GF109203X (2 μM; a PKC inhibitor) were administered 1 min prior to 100 μM esculetin. The data show PMA, GF109203X, nifedipine, econazole or SKF96365 hampered esculetin-provoked $[Ca^{2+}]_i$ raises by 50% ($P < 0.05$) (Fig. 4).

Sources of esculetin-provoked Ca^{2+} release

ER is known to be the major Ca^{2+} depot [19] in cells. Hence the part ER played in esculetin-provoked Ca^{2+} discharge in PC3 cells was examined. The assays were conducted in Ca^{2+}-free solution to keep out participation of Ca^{2+} entry. Figure 5(**a**) suggest administration of 1 μM thapsigargin [20], a selective ER Ca^{2+} pump suppressor, provoked $[Ca^{2+}]_i$ raises of 25 ± 2 nM. Administration of 100 μM esculetin at 500 s failed to cause $[Ca^{2+}]_i$ raises. On the other hand, Fig. 5(**b**) illustrates after 100 μM esculetin-provoked $[Ca^{2+}]_i$ raises, administration of 1 μM thapsigargin at 500 s still provoked $[Ca^{2+}]_i$ raises with a magnitude similar to control.

Involvement of phospholipase C (PLC) in esculetin-provoked $[Ca^{2+}]_i$ raises

PLC is a crucial protein that regulates the discharge of Ca^{2+} from Ca^{2+} depository. Since esculetin discharged Ca^{2+} from ER, the part PLC plays in this event was investigated. The PLC inhibitor U73122 [21], was used to survey if U73122 was necessary for esculetin-caused Ca^{2+} discharge [22, 23]. Figure 6(**a**) illustrates ATP (10 μM) provoked $[Ca^{2+}]_i$ raises of 49 ± 2 nM at 200 s. ATP is a PLC-associated stimulant of $[Ca^{2+}]_i$ raises [24], and hence was used to examine whether U73122 successfully suppressed PLC. Figure 6(**b**) suggests treatment with 2 μM U73122 fell short to alter resting $[Ca^{2+}]_i$, but completely suppressed ATP-provoked $[Ca^{2+}]_i$ raises. This demonstrated that U73122 successfully repressed PLC. The data further implicated treatment with 2 μM U73122 failed to change resting $[Ca^{2+}]_i$ but totally inhibited 100 μM esculetin-provoked $[Ca^{2+}]_i$ raises ($P < 0.05$). U73343 (2 μM), an inert analogue with a structure similar to U73122, did not inhibit ATP-provoked $[Ca^{2+}]_i$ raises (unshown).

Esculetin reduced cell viability dose-dependently

WST-1 assays were applied in the presence of different doses of esculetin to analyze cell death. Cells were incubated with 0–70 μM esculetin overnight, and data show cells were killed in a dose-dependent fashion between 20–70 μM (Fig. 7). We determined whether esculetin-provoked death was elicited by $[Ca^{2+}]_i$ raises. The cytosolic Ca^{2+} binder BAPTA/AM (5 μM) [25] was utilized to avoid $[Ca^{2+}]_i$ raises during esculetin treatment. At 100 μM, esculetin fell short to provoke $[Ca^{2+}]_i$ raises in BAPTA/AM-treated cells (not shown). Figure 7 demonstrates that 5 μM BAPTA/AM treatment fell short to inhibit control cell viability. In the company of 20–70 μM esculetin, BAPTA/AM incubation did not thwart esculetin-provoked cytotoxicity.

Discussion

Ca^{2+} movement modulates cell physiology [26]. Whether esculetin influences Ca^{2+} movement in PC3 cells is unknown. Esculetin provoked $[Ca^{2+}]_i$ raises in cells dose-dependently at 25–100 μM. Esculetin provoked $[Ca^{2+}]_i$ raises by emptying Ca^{2+} depots and provoking Ca^{2+} entry since removing external Ca^{2+} reduced 100 μM esculetin-provoked $[Ca^{2+}]_i$ raises by 15%. This implicated Ca^{2+} influx and Ca^{2+} discharge

occurred during 220 s of recording. It seems Ca^{2+} influx was via the store-operated Ca^{2+} channels because of the inhibition of esculetin-provoked $[Ca^{2+}]_i$ raises by nifedipine, econazole and SKF96365. These reagents are regularly utilized as inhibitors of this Ca^{2+} entry [27–29]. Nevertheless, there are no specific inhibitors available [30, 31].

PKC modulators, nifedipine, SKF96365, and econazole inhibited 50% of the response-provoked by 100 μM esculetin. This implicates these modulators not only totally blocked Ca^{2+} influx, but also inhibited some portion of Ca^{2+} discharge from ER. The action of kinases is thought to couple with Ca^{2+} handling [32]. In the same vein, in PC3 cells, diindolylmethane- and resveratrol-provoked Ca^{2+} entry involved PKC-modulated store-operated Ca^{2+} entry [33, 34].

Regarding Ca^{2+} depository that participated in esculetin-provoked Ca^{2+} discharge, the thapsigargin-sensitive ER depots seem to be the main one. Because esculetin did not affect thapsigargin-provoked Ca^{2+} discharge, it appears that although both esculetin and thapsigargin discharged Ca^{2+} from ER, the thapsigagin-sensitive Ca^{2+} depository is much larger than that sensitive to esculetin. The data also depict Ca^{2+} discharge was through a PLC-associated route, given the discharge was completely suppressed when PLC was suppressed. Thus the results imply that esculetin evoked Ca^{2+} discharge from ER in a manner dependent on PLC. Our results implicate esculetin provoked death in PC3 cells at concentrations akin to that provoking $[Ca^{2+}]_i$ raises.

I has been shown (7) that 75 μM esculetin caused apoptosis by 6.25% in PC3 cells incubated for 48 h in WST-1 whereas our data show that incubation of 70 μM esculetin overnight killed nearly 95% of PC3 cells. Thus it appears different methodology produced different results. The cytotoxic effect of esculetin on viability of PC3 cells is controversial. Esculetin was reported not to alter cell viability in PC3 cells (35).

Note that in $[Ca^{2+}]_i$ experiments esculetin at 25–100 μM was not cytotoxic, whereas in cytotoxicity experiments, 20–70 μM esculetin killed cells dose-dependently. This was because $[Ca^{2+}]_i$ assays were terminated within 20 min, and cytotoxicity assays were conducted after overnight incubation for WST-1 to act. This cytotoxic action seems to be dissociated of $[Ca^{2+}]_i$ raises since BAPTA/AM incubation suppressed 100 μM esculetin-provoked $[Ca^{2+}]_i$ raises, but did not reverse cytotoxicity (11). Cytotoxic action could be Ca^{2+}-associated or -dissociated (10,36). In PC3 cells, Chang et al (10) suggested resveratrol provoked cell proliferation in a Ca^{2+}-associated fashion. Conversely, Tsai et al (33) illustrated diindolylmethane provoked cell death in a Ca^{2+}-dissociated fashion.

Collectively, in PC3 cells, esculetin provoked Ca^{2+} influx through PKC-modulated store-operated Ca^{2+} channels and Ca^{2+} discharge from ER in a PLC-associated manner. Esculetin provoked Ca^{2+}-dissociated death. The effect of esculetin on Ca^{2+} signaling and death in other cells merits further investigation.

Declarations

Funding

We thank Kaohsiung Veterans General Hospital (KSVGH110-109) granted to WJL for supporting this study.

Author contributions

JLW, WCL, RAL gave effort to the plan of study and conducted assays; SHC, CCK contributed to collecting data; LJH managed manuscript preparation; CTC perform the analysis of statistics; CRJ supervised the whole process of manuscript preparation.

Data availability

Data are fully accessible.

Conflict of interest

No conflicts of interest were declared.

Consent to participate

Authors consent to participate.

Consent for publication

Authors agree to publish.

Ethical approval

This work does not have participation of human participants or animals.

References

1. Liang C, Ju W, Pei S, Tang Y, Xiao Y (2017) Pharmacological Activities and Synthesis of Esculetinand Its Derivatives: A Mini-Review Molecules 22:387.
2. Kadakol A, Sharma N, Kulkarni YA, Gaikwad AB (2016) Esculetin: A phytochemical endeavor fortifying effect against non-communicable diseases. Biomed Pharmacother 84:1442-1448.
3. Li J, Li S, Wang X, Wang H (2017) Esculetininduces apoptosis of SMMC-7721 cells through IGF-1/PI3K/Akt-mediated mitochondrial pathways. Can J Physiol Pharmacol 95:787-794.
4. Zhu X, Gu J, Qian H (2018) EsculetinAttenuates the Growth of Lung Cancer by Downregulating Wnt Targeted Genes and Suppressing NF-κB. Arch Bronconeumol 54:128-133.
5. Rubio V, García-Pérez AI, Herráez A, Tejedor MC, José C Diez JC (2017) Esculetinmodulates cytotoxicity induced by oxidants in NB4 human leukemia cells. Exp Toxicol Pathol 69:700-712.

6. Wang G, Lu M, Yao Y, Wang J, Li J (2017) Esculetinexerts antitumor effect on human gastric cancer cells through IGF-1/PI3K/Akt signaling pathway. Eur J Pharmacol 814:207-215.
7. Turkekul K, Colpan RD, Baykul T, Ozdemir MD, Erdogan S (2018) EsculetinInhibits the Survival of Human Prostate Cancer Cells by Inducing Apoptosis and Arresting the Cell Cycle. J Cancer Prev 23:10-17.
8. Arora R, Sawney S, Saini V, Steffi C, Tiwari M, Daman Saluja D (2016) Esculetininduces antiproliferative and apoptotic response in pancreatic cancer cells by directly binding to KEAP1. Mol Cancer 15:64.
9. Kim AD, Han X, Piao MJ, SRKMHewage, Hyun CL, Cho SJ, Hyun JW (2015) Esculetin induces death of human colon cancer cells via the reactive oxygen species-mediated mitochondrial apoptosis Environ Toxicol Pharmacol 39:982-989.
10. Chang HT, Chou CT, Lin YS, Pochuen Shieh P, Kuo DH, Jan CR, Liang Wei-Zhe (2016) Esculetin, a natural coumarin compound, evokes Ca^{2+} movement and activation of Ca^{2+}-associated mitochondrial apoptotic pathways that involved cell cycle arrest in ZR-75-1 human breast cancer Tumour Biol 37:4665-4678.
11. Berridge MJ (2016) The Inositol Trisphosphate/Calcium Signaling Pathway in Health and Disease. Physiol Rev 96:1261-1296.
12. BootmanMD, Allman S, Rietdorf K, Bultynck (2018) Deleterious effects of calcium indicators within cells; an inconvenient truth. Cell Calcium 73:82-87.
13. Thor K (2019) Calcium-Nutrient and Messenger. Front Plant Sci 10:440.
14. Ong HL, Ambudkar IS (2017) STIM-TRP Pathways and Microdomain Organization: Contribution of TRPC1 inStore-Operated Ca^{2+} Entry: Impact on Ca^{2+} Signaling and Cell Function. Adv Exp Med Biol 993:159-188.
15. Shigeto M, Cha CY, Rorsman P, Kohei Kaku (2017) A role of PLC/PKC-dependent pathway in GLP-1-stimulated insulin secretion. J Mol Med (Berl) 95:361-368.
16. Cui C, Merritt R, Fu L, Pan Z (2017) Targeting calcium signaling in cancer therapy. Acta Pharm Sin B7:3-17.
17. Grynkiewicz G, Poenie M, Tsien RY (1985) A new generation of Ca^{2+} indicators with greatly improved fluorescence properties. J Biol Chem 260:3440-3450.
18. Merritt JE, Jacob R, Hallam TJ (1989) Use of manganese to discriminate between calcium influx and mobilization from internal stores in stimulated human neutrophils. J Biol Chem 264:1522-1527.
19. Bootman MD, Berridge MJ, Roderick HL (2002) Calcium signalling: more messengers, more channels, more complexity. Curr Biol 12:R563-R565.
20. Thastrup O, Cullen PJ, Drøbak BK, Hanley MR, Dawson AP (1990) Thapsigargin, a tumor promoter, discharges intracellular Ca^{2+} stores by specific inhibition of the endoplasmic reticulum Ca^{2+}-ATPase. Proc Natl Acad Sci USA 87:2466-2470.

21. Thompson AK, Mostafapour SP, Denlinger LC, Bleasdale JE, Fisher SK (1991) The aminosteroid U-73122 inhibits muscarinic receptor sequestration and phosphoinositide hydrolysis in SK-N-SH neuroblastoma cells. A role for Gp in receptor compartmentation. J Biol Chem 266:23856-23862.
22. Diambra L, Marchant JS (2009) Localization and socialization: experimental insights into the functional architecture of IP3 Chaos 19:037103.
23. Heemskerk JW, Farndale RW, Sage SO (1997) Effects of U73122and U73343 on human platelet calcium signalling and protein tyrosine phosphorylation. Biochim Biophys Acta 1355:81-88.
24. Florenzano F, Viscomi MT, Mercaldo V, Longone P, Bernardi G, Bagni C, Molinari M, Carrive P (2006) P2X2R purinergic receptor subunit mRNA and protein are expressed by all hypothalamic hypocretin/orexin neurons. J Com Neurol 498:58-6
25. Tsien RY (1980) New calcium indicators and buffers with high selectivity against magnesium and protons: design, synthesis, and properties of prototype structures. Biochemistry 19:2396-2404.
26. Berridge MJ (2002) The endoplasmic reticulum: a multifunctional signaling organelle. Cell Calcium 32:235-249.
27. Carrillo C, Giraldo M, Cavia MM, Sara R Alonso-Torre SR (2017) Effect of oleic acid on store-operatedcalcium entry in immune-competent cells. Eur J Nutr 56:1077-1084.
28. Dago CD, Maux PL, Roisnel T, Brigaudeau C, Bekro YA, Olivier Mignen O, Bazureau JP. Preliminary Structure-Activity Relationship (SAR) of a Novel Series of Pyrazole SKF-96365 Analogues as Potential Store-OperatedCalcium Entry (SOCE) Inhibitors. Int J Mol Sci 2018;19: 856.
29. Jin Zhang, W Gil Wier, Mordecai P Blaustein (2002) Mg^{2+} blocks myogenic tone but not K+-induced constriction: role for SOCs in small arteries Am J Physiol Heart Circ Physiol 283:H2692-H2705.
30. Rohacs T (2013) Regulation of transient receptor potential channels by the phospholipase C pathway. Adv Biol Regul 53:341-355.
31. Bynagari-Settipalli YS, Lakhani P, Jin J, Bhavaraju K, Rico MC, Kim S, Woulfe D, Kunapuli SP (2012) Protein kinase C isoform ε negatively regulates ADP-induced calcium mobilization and thromboxane generation in platelets. Arterioscler Thromb Vasc Biol 32:1211-1219.
32. Wu-Zhang AX, Newton AC (2013) Protein kinase C pharmacology: refining the toolbox. Biochem J 452:195-209.
33. Tsai JY, Chou CT, Liu SI, Liang WZ, Kuo CC, Liao WC, Lin KL, Hsu SS, Lu YC, Huang JK, Jan CR (2012) Effect of diindolylmethane on Ca^{2+} homeostasis and viability in PC3human prostate cancer cells. J Recept Signal Transduct Res 32:271-278.
34. Chang HT, Chou CT, Chen IL, et al. Mechanisms of resveratrol-induced changes in $[Ca^{2+}]_i$ and cell viability inPC3 human prostate cancer cells. J Recept Signal Transduct Res 2013; 33: 298-303.
35. Ondrey F, Harris JE, Anderson KM (1989) Inhibition of U937 eicosanoid and DNA synthesis by 5,8,11,14-eicosatetraynoic acid, an inhibitor of arachidonic acid metabolism and its partial reversal by leukotriene C4. Cancer Res 49:1138-1142.

36. Ray SD, Sorge CL, Kamendulis LM, Corcoran GB (1992) Ca^{2+}-activated DNA fragmentation and dimethylnitrosamine-induced hepatic necrosis: effects of Ca^{2+}-endonuclease and poly(ADP-ribose) polymerase inhibitors in mice. J Pharmacol Exp Ther 263:387-394.

Figures

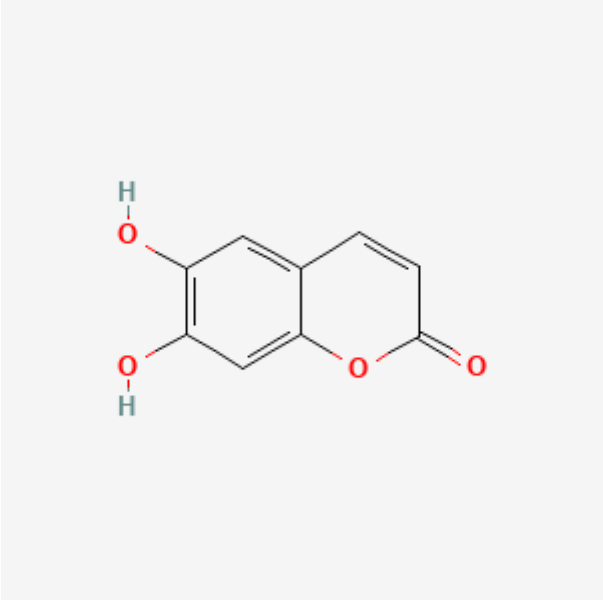

Figure 1

Chemical structure of esculetin.

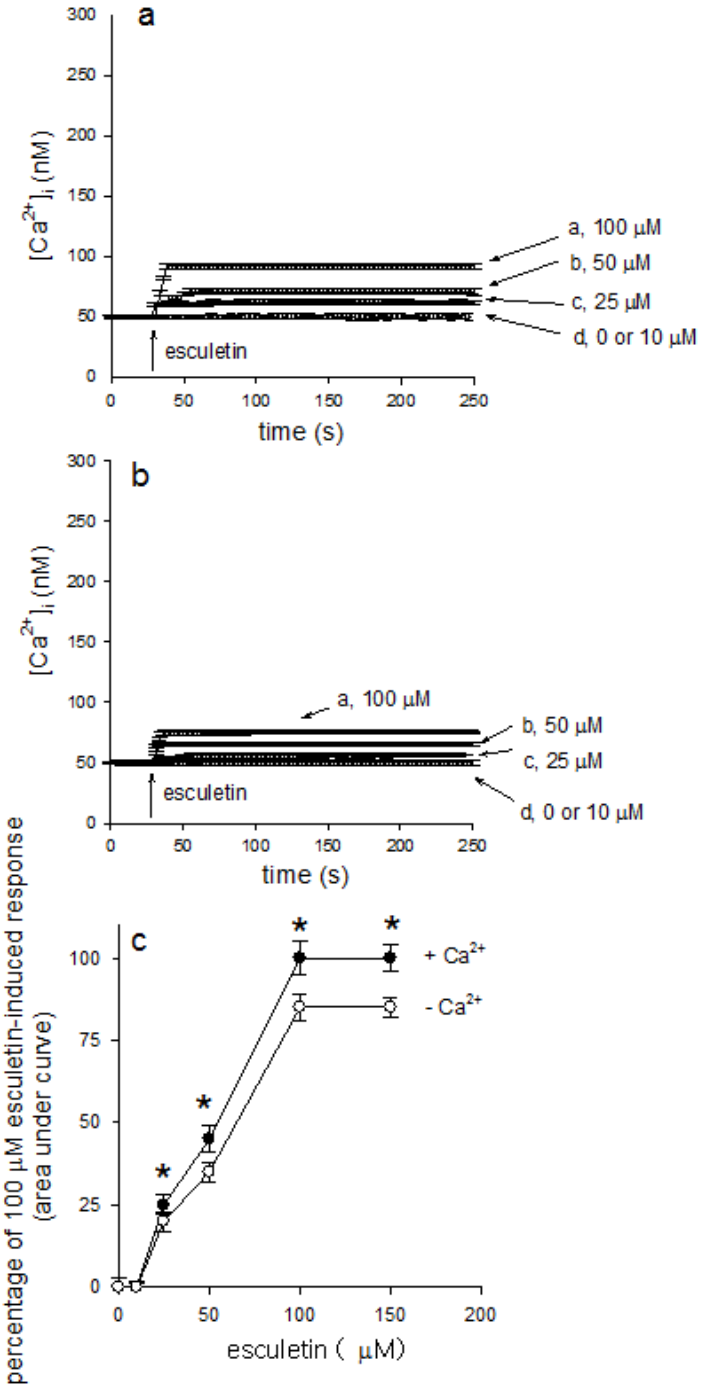

fig 2

Figure 2

Action of esculetin on Ca2+ signaling in fura-2-loaded cells. (a) Esculetin provoked [Ca2+]i raises . Esculetin was administrated at 25 s. The dose of esculetin was shown. The assays were conducted in the presence of Ca2+. (b) Action of esculetin on [Ca2+]i in the absence of Ca2+. Esculetin was administrated at 25 s in the absence of Ca2+. (c) Dose-signal relationships of esculetin-provoked [Ca2+]i raises. Y axis is the percentage of the net area under the recording (25-250 s) of the [Ca2+]i raises provoked by 100 μM

esculetin in the presence of Ca2+ (control). Results are mean ± standard deviation from three unrelated assays. *P < 0.05 in comparison to filled circles.

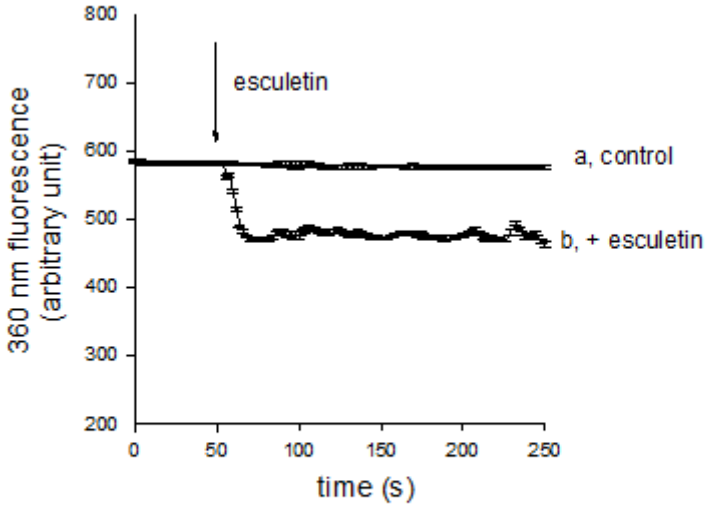

fig 3

Figure 3

Action of esculetin on Ca2+ entry by detecting Mn2+ smothering of fluorescence. Assays were conducted in the presence of Ca2+. MnCl2 (50 μM) was administrated to cells 1 min prior to assays. The y axis is fluorescence intensity (in random units) recorded at the Ca2+-insensitive excitation wavelength of 360 nm and the emission wavelength of 510 nm. Trace a: without esculetin. Trace b: with esculetin (100 μM). Results are mean ± standard deviation from three unrelated assays.

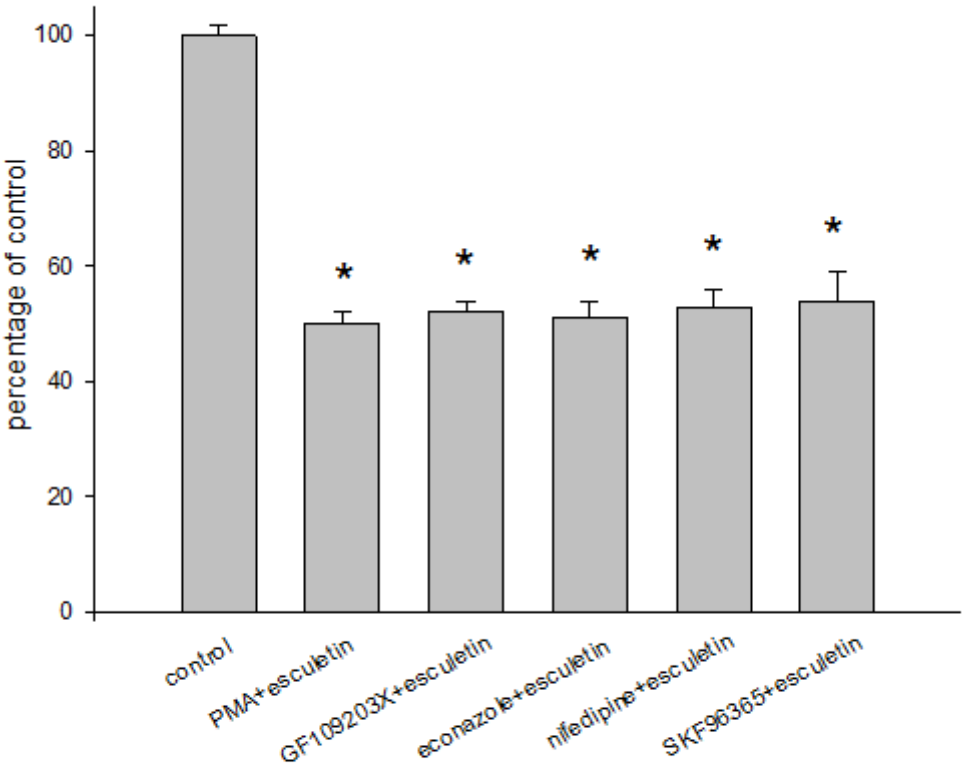

fig 4

Figure 4

Action of Ca2+ channel regulators on esculetin-provoked [Ca2+]i raises. In blocker- or modulator-pretreated groups, the compound was administrated 1 min prior to esculetin (100 μM). The dose was 10 nM for phorbol 12-myristate 13-acetate (PMA), 2 μM for GF109203X, 1 μM for nifedipine, 0.5 μM for econazole, 5 μM for SKF96365. Results are presented as the percentage of control (1st column) that is the area under the recording (25-200 s) of 100 μM esculetin-provoked [Ca2+]i raises. Results are mean ± standard deviation from three unrelated assays. *P < 0.05 in comparison to 1st column.

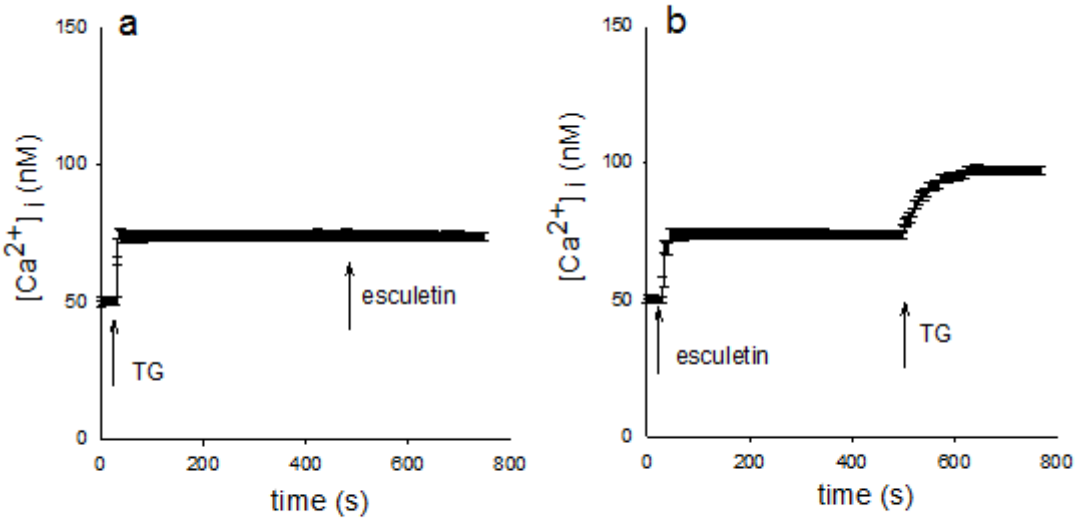

fig 5

Figure 5

Action of thapsigargin on esculetin-provoked Ca2+ discharge. (a)(b) Thapsigargin (TG; 1 μM) and esculetin (100 μM) were administrated at time depicted. Assays were conducted in the absence of Ca2+. Results are mean ± standard deviation from three unrelated assays.

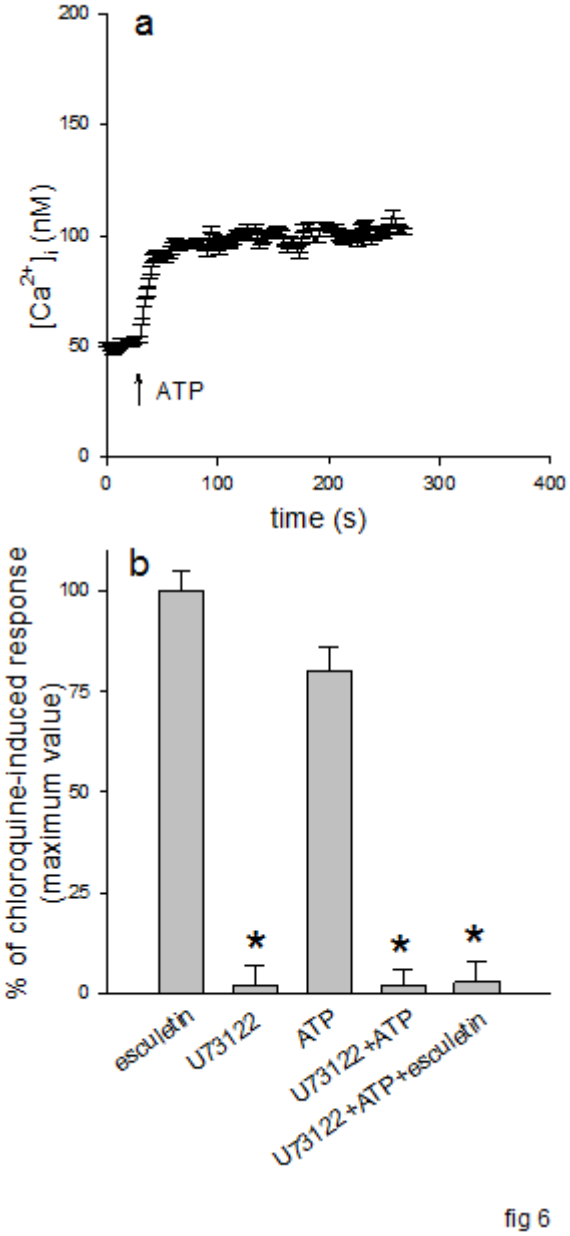

Figure 6

Ation of U73122 on esculetin-provoked Ca2+ discharge. Assays were conducted in the absence of Ca2+. (a) ATP (10 μM) was administered as shown. (b) 1st column is 100 μM esculetin-provoked [Ca2+]i raises. 2nd depicts that 2 μM U73122 fell short to change resting [Ca2+]i. 3rd column illustrated ATP-provoked [Ca2+]i raises. 4th column confirms that U73122 treatment for 1 min totally suppressed ATP-provoked [Ca2+]i raises (*P<0.05 in comparison to 3rd column). 5th column depicts that U73122 (treatment for 1 min) and ATP (treatment for 30 s) treatment suppressed 100 μM esculetin-provoked [Ca2+]i raises. Results are mean ± standard deviation from three unrelated assays. *P < 0.05 in comparison to 1st bar (control). Control is the area under the recording of 100 μM esculetin-provoked [Ca2+]i raises (25-220 s).

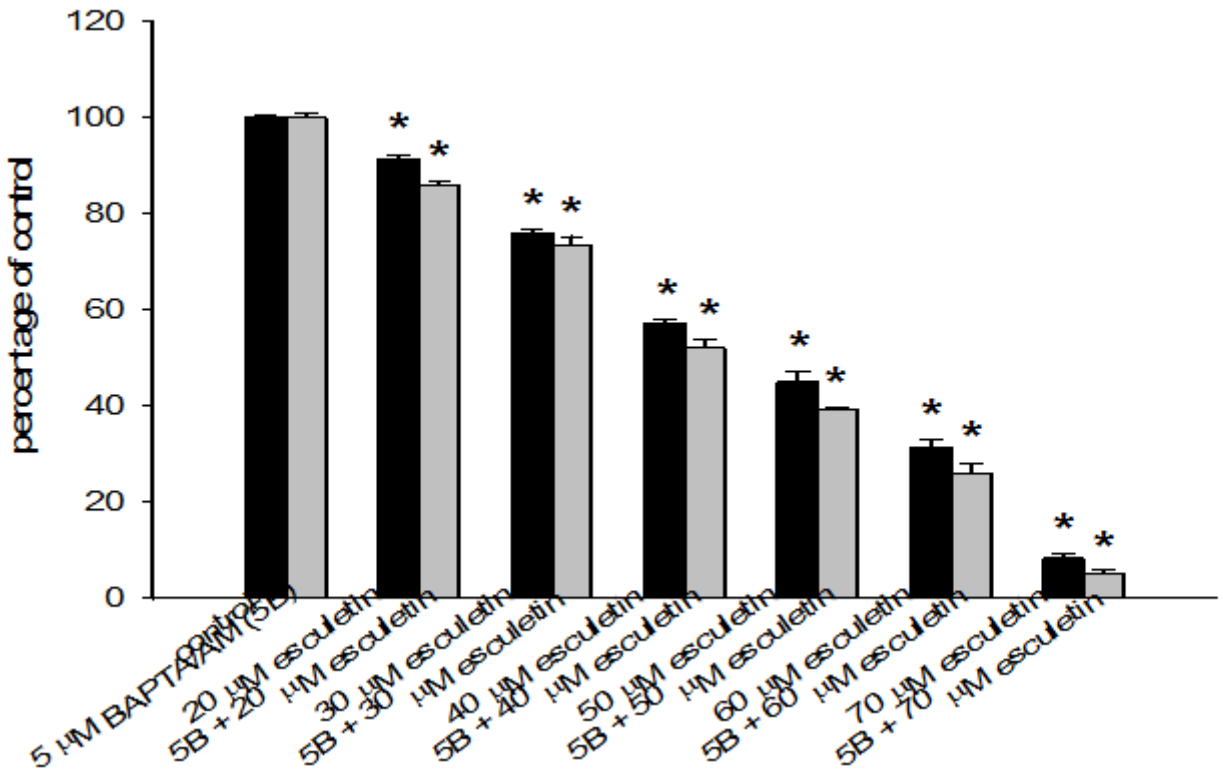

Figure 7

Action of esculetin on cytotixicity. Cells were pretreated with 0-70 μM esculetin for 24 h, and the WST-1 assays were conducted. Results are presented as percentage of control that is the increase in cell numbers in esculetin-free groups. Control had 10,811 ± 180 cells/well before assays, and had 13,488 ± 155 cells/well after incubation overnight. In each group, the Ca2+ binding agent BAPTA/AM (5 μM) was administrated to cells prior to pretreatment with esculetin in the presence of Ca2+. Cell viability analysis was then conducted. Results are mean ± standard deviation from three unrelated assays. *P < 0.05 in comparison to control.